

UNCLASSIFIED

AD NUMBER

ADA182288

LIMITATION CHANGES

TO:

Approved for public release; distribution is unlimited.

FROM:

Distribution authorized to U.S. Gov't. agencies and their contractors;
Administrative/Operational Use; 1987. Other requests shall be referred to Office of Naval Research, 875 North Randolph Street, Arlington, VA 22203-1995.

AUTHORITY

ONR code 1132SM, ltr, 10 Jun 1987

THIS PAGE IS UNCLASSIFIED

UCLA School of Engineering and Applied Science

Department of Civil Engineering

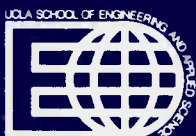
UCLA-ENG-87-11

Interaction of Two Slip Planes on Extrusion Growth in Fatigue Band

The report was sponsored by the Office of Naval Research
through contract N00014-86-K0153

California University, Los Angeles.

T.H. Lin*
S.R. Lin**
X.Q. Wu*



Interaction of Two Slip Planes
on
Extrusion Growth in Fatigue Band

T.H. Lin*
S.R. Lin**
X.Q. Wu*

* Department of Civil Engineering, University of California, Los Angeles

**Structural Technology Office, The Aerospace Corporation, El. Segundo, California 90245-2691

1987 (?)

This research described in this report was sponsored by
the Office of Naval Research through contract N00014-
86-K0153

Abstract

Micromechanic theory of fatigue crack initiation by Lin and his associates is reviewed. Intrusions and extrusions have been observed in fatigue specimens. An initial stress field favorable for the growth of extrusion or intrusion can be produced by arrays of dislocation dipoles as shown by Lin (1969). These dipoles cause an initial tensile strain giving an elongation which is called the static extrusion. It has been suggested that after extrusion reaches the height of static extrusion, extrusion growth terminates. Along the direction of an extrusion, tensile strain and tensile stress occurs. This tensile stress causes the resolved shear stress to reach critical and slide in a secondary slip system. The slip causes plastic tensile strain which increases significantly the extrusion growth. Similarly the same mechanism exists for the growth of intrusions. This explains why extrusion grows much more than the static extrusion.

Introduction

McCommon & Rosenberg [1] and MacCrone et al. [2] show that metal are subject to fatigue at temperature as low as $1.7^{\circ}k$. This seems to indicate that although surface corrosion, gas adsorption, gas diffusion into the metal or vacancy diffusion to form voids can have important effect on but are not necessary to the fatigue crack initiation. Local plastic deformation resulting from the displacement of dislocation generally proceeds this initiation.

Forsyth and Stubbington 1954 [3] reported the detection of extrusion in slip bands during fatigue of some aluminum alloys. Thompson, Wadsworth and Louat [4] and Hull [5] detected the extrusion process in both copper and aluminum. This initiation of extrusion process was also observed by Meke and Blochwitz [6] and Mughrabi [7] in their studies of persistent slip bands.

Following the clue, which the observation on extrusions and intrusions in slip bands have provided, a number of theories of fatigue crack initiation have been proposed by different distinguished investigators. For example, Mott [8] proposed that a screw dislocation repeats its path through cross slip. He considered a column of metal containing a single screw dislocation intersecting a free surface. When this dislocation travels a complete circuit, the volume contained in the circuit is translated parallel to the dislocation. This causes the metal to extrude. This mechanism does not explain why the dislocation under cyclic stressing, does not oscillate back and forth along the same path rather than traversing a closed circuit. Clearly some form of gating mechanism is required to convert the back and forth oscillations of screw dislocations into unidirectional circuits. Cottrell and Hull [9] proposed that Frank Read sources exist on two intersecting slip planes and a complete cycle of forward and reversed loading results in an extrusion and intrusion. Such a model would predict the extrusion and intrusion to form in neighboring slip bands and to be inclined to each other, but they have been found to occur in the same slip band and to be parallel to each other. Thompson

[10] proposed an edge-screw interaction model for the initiation of extrusion. This model assumes a change of spacing of a pair of parallel screw dislocations after being cut an edge dislocation. This cut causes jogs in both edge and the screw dislocations and this cut will inhibit the change of the spacing of the pair of screw dislocations [11]. It is also hard to see how intrusions are formed by such a model. McEvily and Machlin [12] proposed a model, in which two screw dislocations terminate in a surface and intersect a node where three dislocations meet. Under an alternating shear stress, the two screw dislocations are assumed to shift around a circuit causing an intrusion and an extrusion formed in the same slip band. However, this model as pointed out by Kennedy does not explain why these two dislocations travel around a circuit instead of back and forth. Wood [13] proposed a simple model of a single operative slip system. An unidirectional stressing causes layers of metal to slide in the same direction; but forward and reverse stressing causes different amounts of net slip on different planes and results in peaks and valleys. However, this model and other models of random slip do not explain why, under an alternate loading, the slip continues to monotonically deepen the valley and raise the peaks as observed in experiments. Drawbacks of other theories have also been discussed by Kennedy [11].

For a dislocation to glide, it (1) must glide along a certain direction on a crystal plane (2) must subject to a resolved shear stress equal or greater than the critical shear stress. The above mentioned theories show the possible paths of dislocation movement to satisfy condition (1) but the resolved shear stress field caused by the dislocation movement that has significant effect on (2) was not considered. In the micromechanic theory developed by Lin and his associates, [14-16], this important effect of this stress field in causing the initiation of extrusion and intrusion is considered.

Dependency of slip on resolved shear stress

Single crystal tests [17] have shown that under stress, slip occurs along certain directions on certain crystal planes. These directions and planes are generally those of maximum atomic density. Slip has been found to depend on the resolved shear stress and not on the normal stress on the sliding plane. This dependency of slip on the resolved shear stress under monotonic loadings has also been found to hold under cyclic loadings [18]. Hence to find the slip in a slip band or fatigue band, we need to determine the resolved shear stress distribution in the metal. To determine this stress field, the following analogy between plastic strain and applied force is used.

Analogy between plastic strain and applied force

The resolved shear stress to cause sliding is called the critical shear stress. When this critical shear stress is reached in some region in a body, slip occurs and causes plastic strain. If the load is removed, plastic strain remains and cause a residual stress field. To find this stress field, the analogy between plastic strain and applied force developed by Lin [19,20] is used. This analogy is briefly reviewed as follows:

Referring to a set of rectangular coordinates, the strain component is composed of the elastic part denoted by single prime and the inelastic part denoted by double prime

$$e_{ij} = e'_{ij} + e''_{ij} \quad (1)$$

Thermal, creep and plastic strains are considered to be the inelastic strain. Neglecting the anisotropy of the elastic constants, the stress is related to the elastic strain as

$$\tau_{ij} = \delta_{ij} \lambda \theta' + 2\mu e'_{ij}, \quad (2)$$

$$\tau_{ij} = \delta_{ij} \lambda (\theta - \theta') + 2\mu (e_{ij} - e''_{ij}),$$

where λ and μ are Lamé's constants, θ is the dilation and θ'' is the inelastic dilation. The condition for equilibrium within a body of volume v is

$$\tau_{ij,j} + F_i = 0 \text{ in } v, \quad (3)$$

where the subscript after the comma denotes differentiation, the repetition of the subscript denotes summation from one to three, and F_i denotes the body force per unit volume along the x_i axis. At any point on the boundary Γ with normal v , the i component of the surface traction per unit area $S_i^{(v)}$, can be written from the condition of equilibrium as

$$S_i^{(v)} = \tau_{ij} v_j \text{ on } \Gamma, \quad (4)$$

where v_j is the cosine of the angle between the normal v and the x_j axis. Substituting (2) into (3) and (4), we obtain

$$\delta_{ij}\lambda\theta_{,j} + 2\mu e_{ij,j} - (\delta_{ij}\lambda\theta''_{,j} + 2\mu e''_{ij,j}) + F_i = 0, \quad (5)$$

$$S_i^{(v)} = v_j [\delta_{ij}\lambda\theta + 2\mu e_{ij} - (\delta_{ij}\lambda\theta'' + 2\mu e''_{ij})] \quad (6)$$

It is seen that $-(\delta_{ij}\lambda\theta''_{,j} + 2\mu e''_{ij,j})$ and $(\delta_{ij}\lambda\theta'' + 2\mu e''_{ij}) v_j$ are equivalent to F_i and $S_i^{(v)}$, in causing the strain field e_{ij} and are here denoted by \bar{F}_i and $\bar{S}_i(v)$ respectively, giving

$$\delta_{ij}\lambda\theta_{,j} + 2\mu e_{ij,j} + F_i + \bar{F}_i = 0, \quad (7)$$

$$S_i(v) + \bar{S}_i^{(v)} = v_j (\delta_{ij}\lambda\theta + 2\mu e_{ij}) \quad (8)$$

Hence, the strain distribution in a body with inelastic strain under external load is the same as that in an elastic body (no inelastic strain) with the additional equivalent body and surface forces \bar{F}_i and $\bar{S}_i(v)$. This reduces the solution of stress field of a body with known inelastic strain distribution to the solution of an identical elastic body with an additional set of equivalent body and surface forces. This gives the same results as Eshelby's famous process of imaginary cutting, relaxing, restoring, welding, relaxing in his noteworthy paper on ellipsoidal inclusions [21].

If there is thermal strain only with thermal coefficient of expansion α and temperature T , we can write

$$e''_{ij} = \delta_{ij}\alpha T; \quad \theta'' = e''_{ii} = 3\alpha T$$

Then the equivalent body and surface forces become

$$\bar{F}_i^I = -(e\lambda + 2\mu)\lambda T_{,i}; \quad \bar{S}_i^V = (3\lambda + 2\mu)\lambda T v_i$$

This is the well-known Duhamel's analogy between temperature gradient and the body force in an elastic medium.

Material Defects and Initial Stress Field

Imperfections like dislocations exist in all metals and cause an initial stress field. Consider a most favorably oriented crystal at a free surface. For a slice of extrusion to form, positive shear deformation must occur on one side of the extrusion and negative shear on the other. The initial stress field τ^I near the surface (Fig. 1) favorable for the initiation of extrusion "R" is one with positive resolved shear stress in P above R and a negative one in Q below R. Such an initial stress field can be provided by an inelastic strain field $e''_{\alpha\alpha}$ in R. Consider this strain to be linear i.e. $e''_{\alpha\alpha,\alpha}$ is constant. This causes a uniform \bar{F}_α in R and hence an initial positive and negative resolved shear stress τ^I in P and Q respectively. It has been pointed out by Lin and Ito [22] that this $e''_{\alpha\alpha}$ can be produced by a row of dislocation dipoles. Recently this type of dislocation dipoles has been observed under microscope in fatigue specimens as indicated by Essmann et al. [23] and Mughrabi [24].

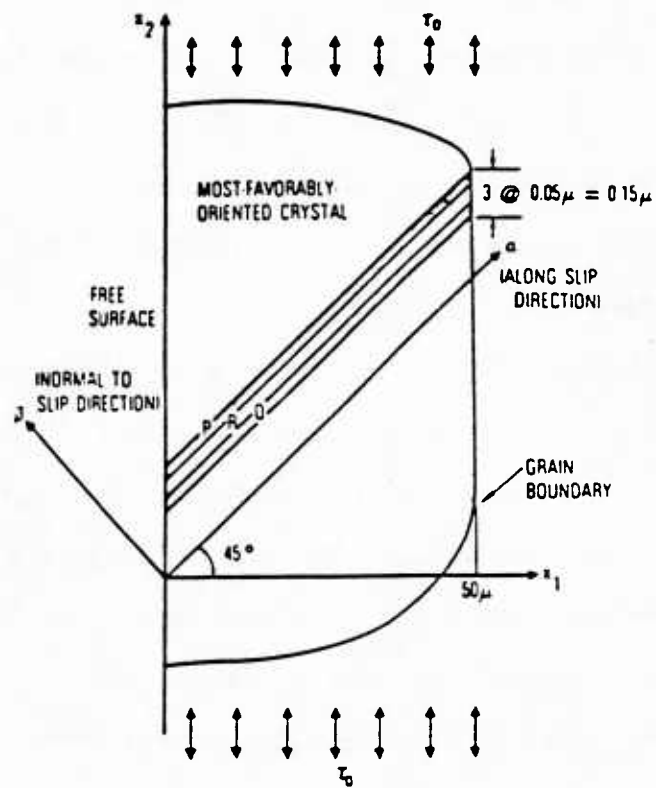


Fig. 1. Most favorably oriented crystal at free surface

A Gating Mechanism

Consider a most favorably oriented crystal at a free surface with such linear $e''_{\alpha\alpha}$ in a polycrystal. A tensile loading causes a uniform resolved shear stress τ^A in the crystal. The signs of the initial shear stress and the applied stress are of the same sign in P and of opposite sign in Q. The stress $\tau^I + \tau^A$ in P is largest in the crystal. Hence P reaches the critical shear stress τ^C first and slides. This causes a residual shear stress τ^R . Due to the continuity of the stress field τ^R , slip in P relieves not only the positive shear stress in P, but also in the neighboring region including Q. This keeps the positive shear stress in the vicinity from reaching that of P and hence from sliding in the tensile loading. This relief of positive shear stress in Q is the same as the increase of negative shear stress. Hence during the compressive loading, Q has the highest negative shear stress and slides. Again this negative slip causes relief of negative shear stress, not only in Q but also in P. This relief of negative shear stress in P is the same as increase of positive shear stress causing P to be more ready to slide in the next tensile loadings. This gives the natural gating mechanism to cause alternate sliding in P and Q. Hence slips in P and Q deepen the valley and raise the peak monotonically as observed in experiments. These microstress fields supply a natural gating mechanism in fatigue bands. With this mechanism, cross-slip is not necessary to supply of irreversible slip as indicated by Mughrabi [25].

Consider the case with positive $e''_{\alpha\alpha}$ and $e''_{\alpha\alpha,\alpha}$. Referring to Fig. 1, the equivalent force \bar{F}_α is pointing outward of the free surface. This caused an extrusion. As the extrusion grows, the thin slice R increases in length. This elongation cause a tensile stress $\tau_{\alpha\alpha}$. For a f.c.c crystal, there are four slip planes. This $\tau_{\alpha\alpha}$ causes the resolved shear stress in another slip system. To simplify the numerical calculation, a second slip system is assumed to have a sliding plane with a normal along x_1 -axis and a sliding direction along x_2 -axis or vice-versa. The resolved shear stress τ_{12} increases with $\tau_{\alpha\alpha}$. After τ_{12} reaches the critical shear stress,

this slip system slides. The slip causes a plastic strain e''_{12} , which causes a plastic tensile strain $e''_{\alpha\alpha}$. Now the total inelastic tensile strain is equal to the sum $e^I_{\alpha\alpha} + e''_{\alpha\alpha}$. This induces large resolved shear stress (initial plus residual) of opposite signs in P and Q, causes a higher rate of extrusion growth, and explains why the fatigue initiation growth rate is higher for f.c.c metals than for hexagonal metals. Some calculations of this secondary slip effect were reported by Lin and Lin [26]

Mughrabi, et. al. [25] have suggested a model of dislocation dipoles in a single crystal as shown in Fig. 2. The initial inelastic strain $e^I_{\alpha\alpha}$ due to the interstitial dipoles is $\frac{mb}{D}$, where m denotes the number of these dipoles. Mughrabi refers to mb as the static extrusion. Cyclic loading causes extrusion to occur on both the right and left ends of the persistent slip band. Part of the static extrusion is lost through the extrusion process. An interesting question which was raised by Mughrabi, and Essmann et. al. [23] was, **after the extrusion has reached the amount of static extrusion , will the extrusion growth process stop?**. Some details of the answer are given in the following analysis.

Now we consider an aluminum polycrystal of fine grain. the grain size is small as compared to the total volume of the aggregate. Hence the inelastic strain in the crystal at the free surface may be considered to be occurring in a semi-infinite medium. Referring to Fig. 1, the thickness of the slices P, Q, and R are much less than the length of the traces of the slip lines on the free surfaces. Consequently, the inelastic strains and their equivalent forces are assumed to be constant along the slip line direction, and the semi-infinite medium is taken to be under plane deformation.

The polycrystal considered is pure aluminum subject to alternate tension and compression τ_0 along x_2 -axis. The resolved shear stress in the most favorably oriented slip system is the same at all points in the crystal.



10

$$\tau_{\alpha\beta}^A(\underline{x}) = \tau_o / 2 \quad (9)$$

The plastic strain e_{ij}'' varies from point to point in the slices P and Q. After slip occurs, a residual stress field is produced. From the plane strain solution of a semi-infinite medium, the stress field is written as

$$\tau_{\alpha\beta}(\underline{x}) = \frac{\tau_o}{2} + \tau_{\alpha\beta}'(\underline{x}) - 2 G \sum_n C(\underline{x}, \alpha\beta; \underline{x}_n, \lambda\beta) e_{\alpha\beta_n}'' \quad (10)$$

where x_n denotes the center point of the nth grid and $e_{\alpha\beta_n}''$ the plastic strain of the nth grid. In the active grids this resolved shear stress equals the critical shear stress τ^C . The local strain hardening in the slip bands is much less than the average macroscopic strain-hardening of the metal. Neglecting this local strain-hardening, and differentiating (10) with respect to τ_o yields

$$\frac{d \tau_{\alpha\beta}(\underline{x})}{d \tau_o} = \frac{1}{2} - 2 G \sum_n C(\underline{x}, \alpha\beta; \underline{x}_n, \alpha\beta) \frac{d e_{\alpha\beta_n}''}{d \tau_o} \quad (11)$$

In active grids, the change of resolved shear stress equals the change of critical shear stress.

This is zero due to the neglect of local strain hardening. Hence

$$2 G \sum_n C(\underline{x}, \alpha\beta; \underline{x}_n, \alpha\beta) \delta e_{\alpha\beta_n}'' = \frac{\delta \tau_o}{2} \quad (12)$$

There are as many unknown $\delta e_{\alpha\beta_n}''$ as there are equations. The plastic strain increments $\delta e_{\alpha\beta_n}''$ in sliding grids for an incremental applied stress $\delta \tau_o$ can be determined. Thin slices P, Q, R as shown in Fig. 1 are taken to be 0.05 μm each along x_2 -axis. The center distance between P, Q is 0.10 μm and the linear dimension of the crystal is take to be 50 μm . For numerical calculation, the crystal is divided into 1010 parallelogram grids oriented 45° to the free surface with 10 equal spacings along x_1 -axis and 101 rows along x_2 -axis. The plastic strain in each grid is assumed to be uniform. The stress field caused by a uniform plastic strain $e_{\alpha\beta}''$ in a grid centered at (x) was calculated. The relief of the resolved shear stress at

(x) due to this $e''_{\alpha\beta}$ is called residual shear stress expressed as

$$\tau_{\alpha\beta}^R(\underline{x}) = 2GC(\underline{x}, \alpha\beta; \underline{x}_n, \alpha\beta) e''_{\alpha\beta_n} \quad (13)$$

where $2GC(\underline{x}, \alpha\beta; \underline{x}_n, \alpha\beta)$ is the resolved shear stress $\tau_{\alpha\beta}$ at \underline{x} due to unit plastic strains $e''_{\alpha\beta}$ at \underline{x}_n . This is called the resolved shear stress influence coefficient. The detail of the calculation of this influence coefficient is shown in by Lin, [27], and Lin & Lin [26].

Effect of Primary Slip on Stress in Secondary Slip

One set of uniform initial shear stress of 24.4 KN/m^2 (3.53 p.s.i) in P and -24.4 KN/m^2 (-3.52 p.s.i.) in Q, and applied tensile and compressive stresses of $\pm 690.0 \text{ KN/m}^2$ (± 100 p.s.i.) was calculated by Lin and Lin, [28]. After 200 cycles, the plastic strain distributed in P,Q were obtained and are shown in Fig. 3. This elastic strain is much less than these plastic ones. Hence these plastic strains represent the total shear strain in P,Q. Let the thickness of P,Q, R be t , then $t = 0.5/\sqrt{2} \mu\text{m}$. The displacement in R along α -direction

$$2(e_{\alpha\beta})_{P,Q} t \cong 2(e''_{\alpha\beta})_{P,Q} t \quad (14)$$

This is similar to shearlag problems in thin wall airplanes structures.

The residual stress $\sigma_{\beta\beta}^R(\underline{x})$ may be expressed as

$$\sigma_{\beta\beta}^R(\underline{x}) = 2GC(\underline{x}, \beta\beta; \underline{x}_n, \alpha\beta) e''_{\alpha\beta_n} \quad (16)$$

Using these influence coefficients, $C(\underline{x}, \beta\beta; \underline{x}_n, \alpha\beta)$ it was found $\sigma_{\beta\beta}^R(\underline{x})$ in R is very small.

$$\sigma_{\beta\beta}^R(\underline{x}) \ll \sigma_{\alpha\alpha}^R(\underline{x}) \quad (17)$$

We have

$$\sigma_{\alpha\alpha} = \frac{E}{1-\nu^2} e_{\alpha\alpha} \quad (18)$$

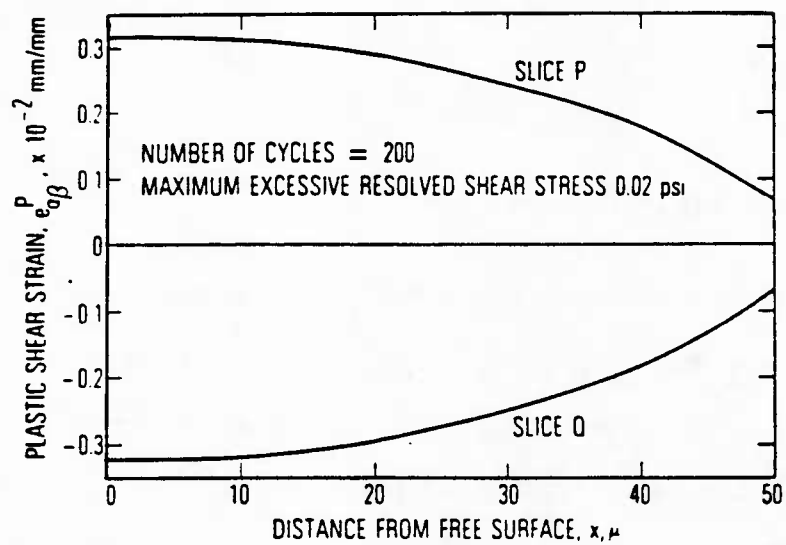


Fig. 3. Plastic Shear Strain Distributions

$$\sigma_{\alpha\alpha}(x) = \frac{E}{1-\nu^2} \left[t \frac{2d}{d\alpha} e''_{\alpha\beta}(x) \right] \quad (19)$$

The resolved shear stress τ_{12} in the secondary slip plane in R is then

$$\tau_{12} = \frac{\sigma_{\alpha\alpha}}{2} \quad (20)$$

Effect of Secondary Slip on Primary Slip

When τ_{12} reaches τ^c in some part of R, e''_{12} occurs in that region. This e''_{12} has a strain component $e''_{\alpha\alpha}$ which adds to the $e^I_{\alpha\alpha}$ in causing the difference in resolved shear stress $\tau_{\alpha\beta}$ in P and Q. This increases the rate of sliding in P,Q thus accelerating the extrusion growth at the free surface as reported by Lin and Lin [26]. This additional $e''_{\alpha\alpha}$ caused by e''_{12} in the second slip system in R causes the extra length of slice R to be more than the initial static extrusion. This is one of the main reasons why the extrusion can proceed on beyond the static extrusion as observed by Essmann et al. [23].

The distribution of e''_{12} in R depends on the variation of slope in $e''_{\alpha\beta}$ in P and Q. The latter depends on the distribution of the initial resolved shear stress in P,Q. To simplify the numerical calculation, it was assumed that only positive slip $e''_{\alpha\beta}$ occurred in P, only negative slip $-e''_{\alpha\beta}$ occurred in Q and only e''_{12} occurred in R. Three cases of initial resolved shear stress were calculated. They are as follows.

- 1) The initial resolved shear stress varies linearly from the interior grain boundary to the free surface

$$\tau^I = \pm 34.5 \frac{KN}{m^2} \left(1 - \frac{x}{d} \right) \quad , + \text{ in } P, \text{ and } - \text{ in } Q.$$

The plastic strains in P,Q are about the same. This distributions of primary slip in P,Q with and without the consideration of the secondary slip in R are shown in Fig. 4. The distribu-

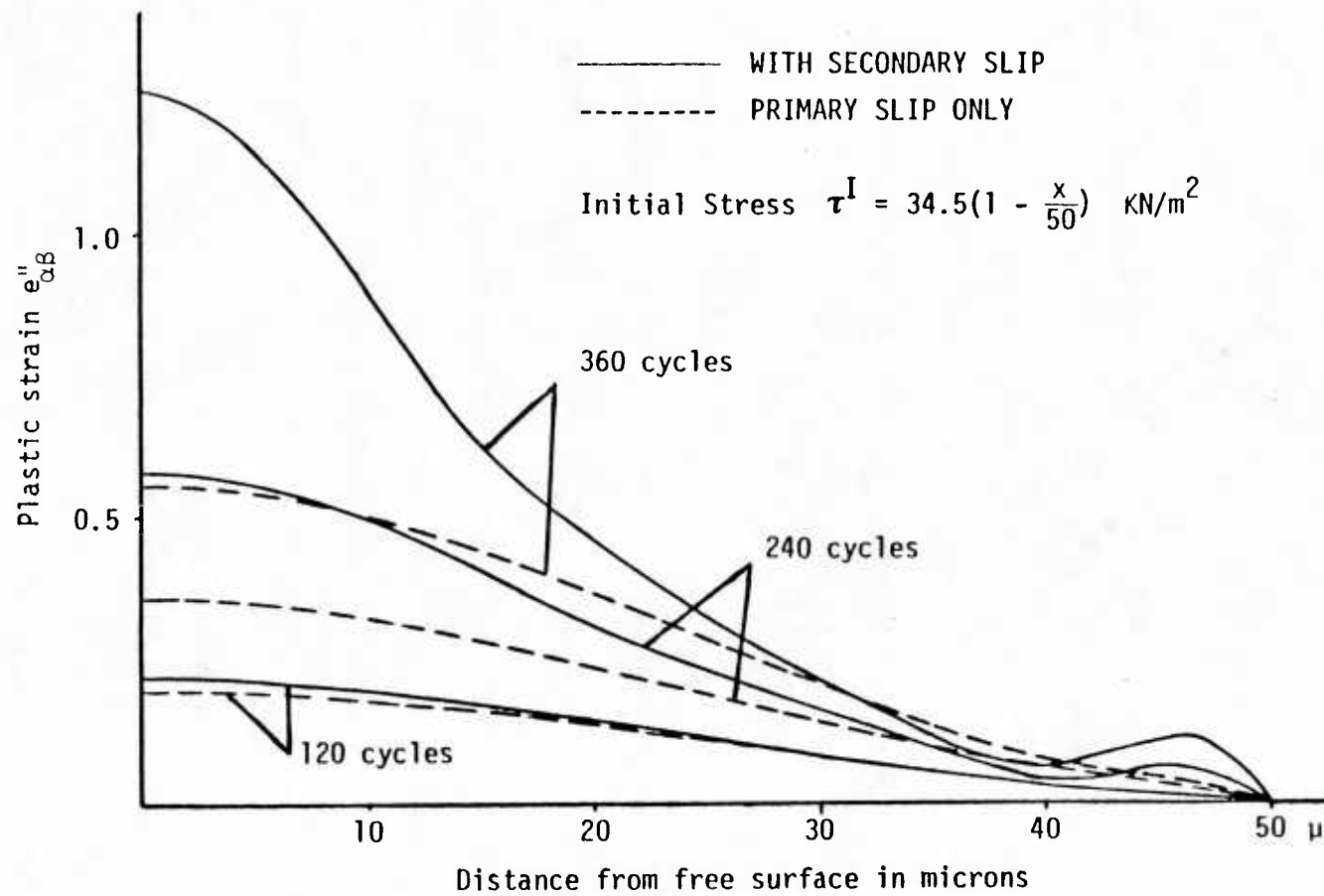


Fig. 4. Plastic Shear Strain $e''_{\alpha\beta}$ in P,Q

tion of the secondary slip in R is shown in Fig. 5. It is to be noted that e''_{12} curve in R is very close to the slope of $e''_{\alpha\beta}$ in P,Q. The equivalent body force caused by e''_{12} is proportional to the slope of e''_{12} curve in R and hence to be the curvature of $e''_{\alpha\beta}$ in P, Q.

2) The initial resolved shear stress in P,Q varies linearly from a maximum value of 3.45 KN/m^2 (5 p.s.i) at the free surface to 13.5 KN/m^2 (2 p.s.i) at the grain boundary. The distributions of the primary slip in P,Q with and without the consideration of the secondary slip in R are shown in Fig. 6. The variation of the secondary slip in R is shown in Fig. 7.

3) The initial resolved shear stress in P,Q varies parabolically from zero (with zero slope) at the grain boundary to a maximum value of 34.5 KN/m^2 (5. p.s.i.) at the free surface. The distribution of the primary slip in P,Q with and without the consideration of the secondary slip in R and shown in Fig. 8. The variation of secondary slip in R is shown in Fig. 9.

The growth of plastic strain $e''_{\alpha\beta}$ at the free surface with cycles of loading for the three cases of initial stresses, with and without secondary slip, is shown in Fig. 10.

Extrapolation Proceedure

The calculation of the secondary slip may require computations for a large number of cycles of loadings. To reduce the computation, an extrapolation proceedure was developed. At the end of the compression loading of the Nth cycle, the incremental plastic strain in P, Q and R in the Nth cycle were calculated and denoted by δe^N . To extrapolate to the (N+n)th cycle, the plastic strains in P were assumed to increase by $n \times \delta e^N$. Since at the end of the (N+n)th cycle, active grids in Q and R just finish sliding and hence have stresses equal to the critical shear stress τ^C . We have

$$\tau^A + \tau^I + \tau^R = \tau_c \quad \text{in } Q \text{ and } R \quad (17)$$

This condition was used to find the incremental plastic strains in Q and R. The number of

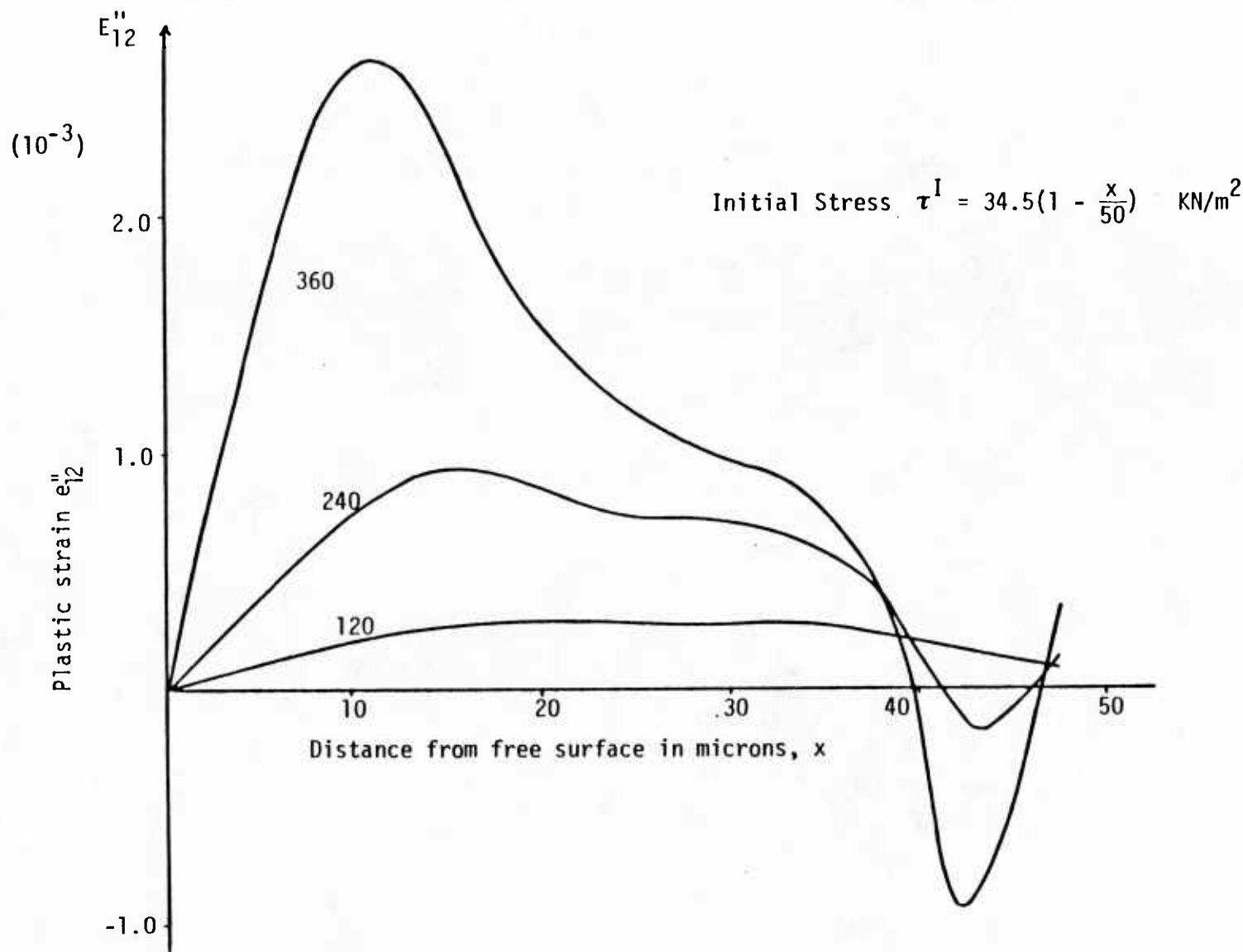


Fig. 5. Plastic Shear Strain e''_{12} in R

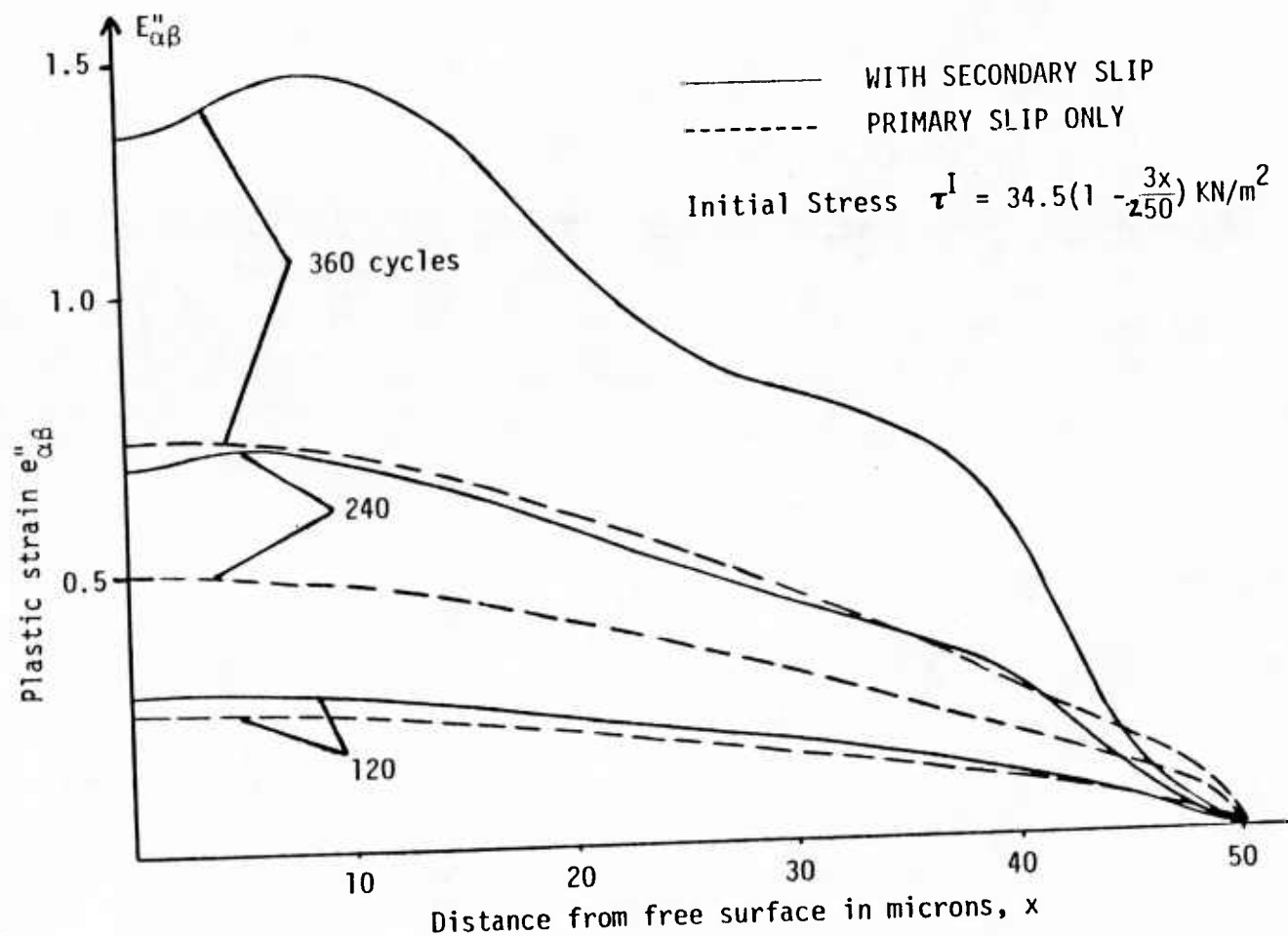


Fig. 6. Plastic Strain Distribution $e''_{\alpha\beta}$ in P,Q

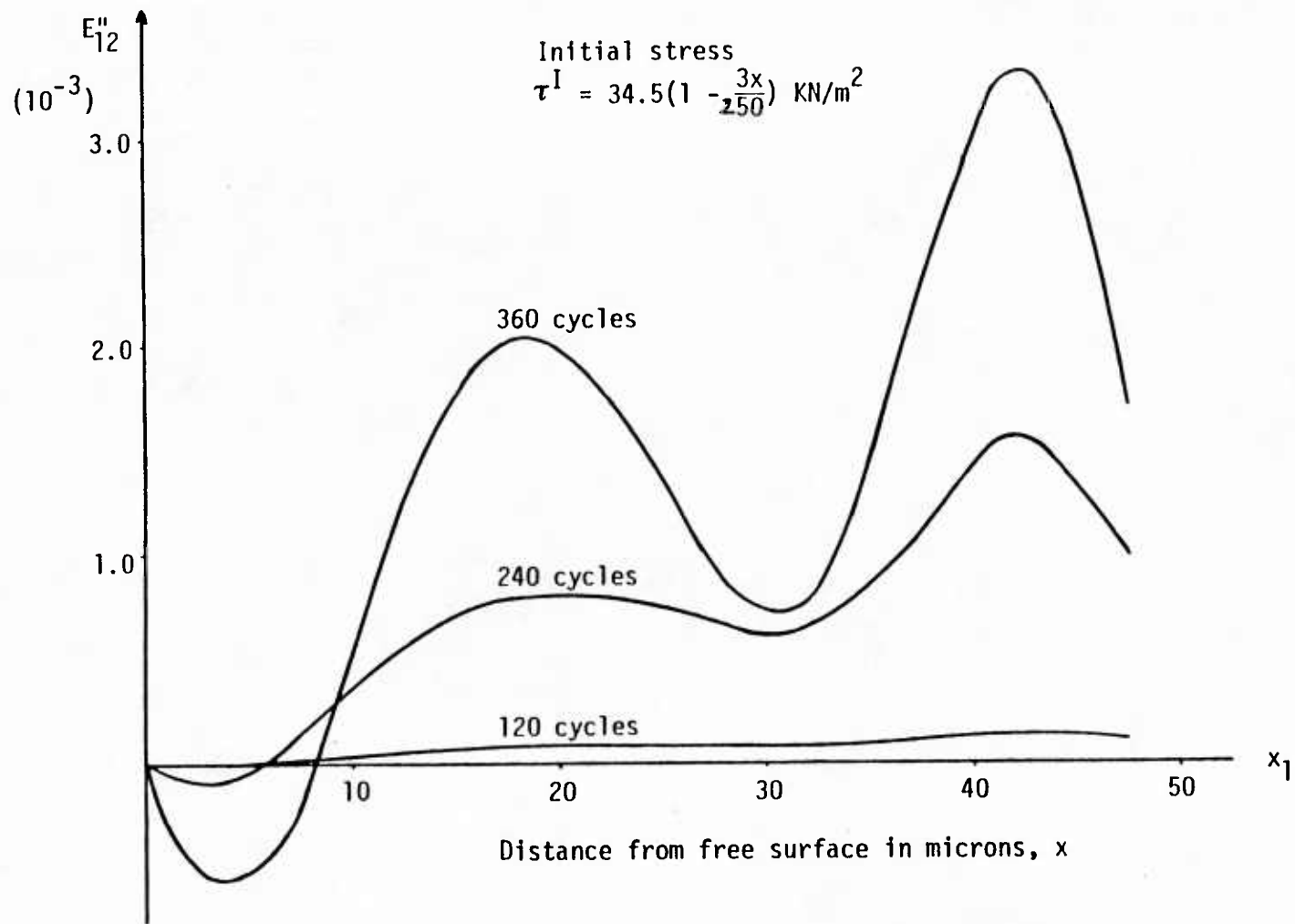
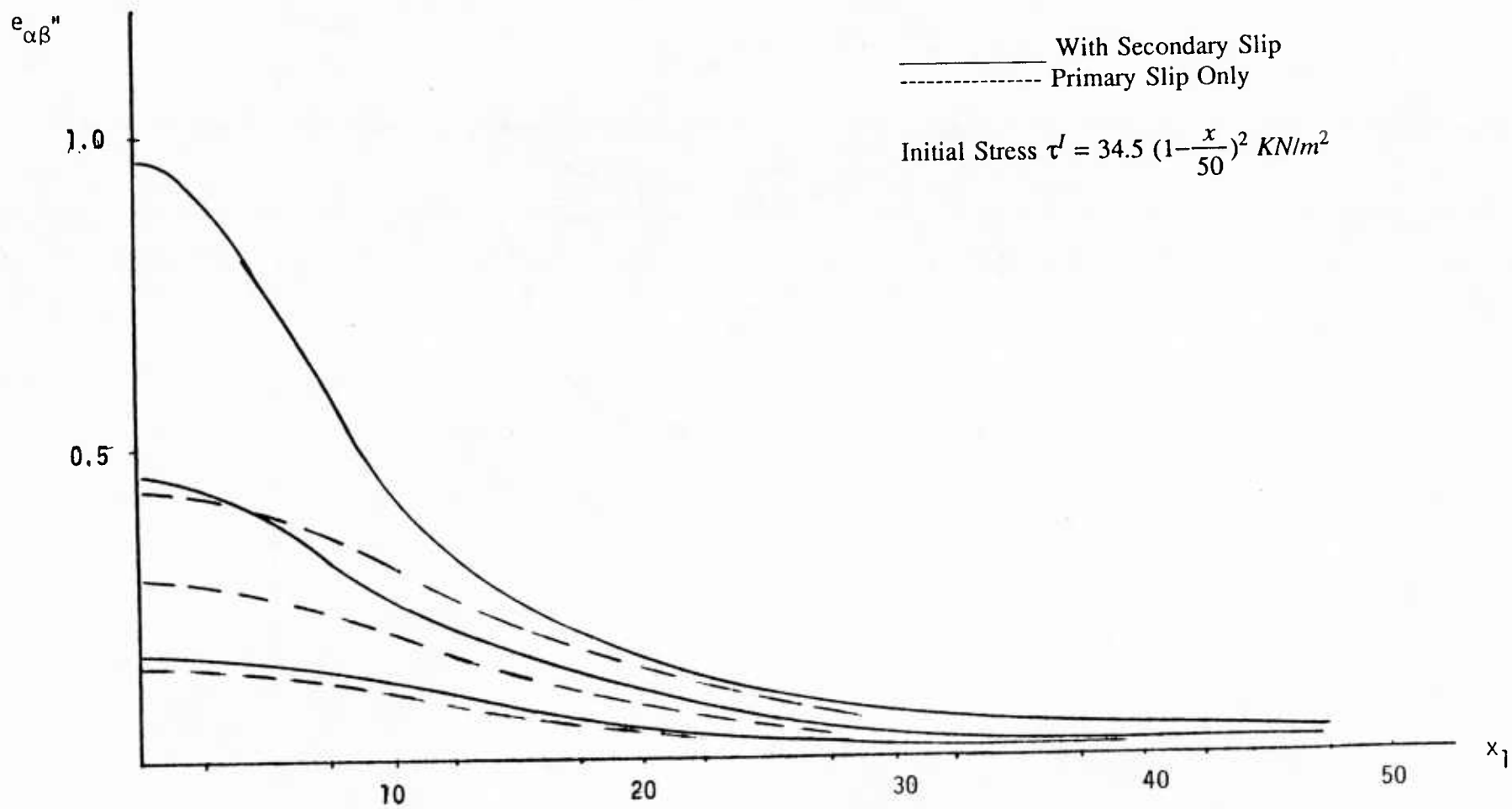
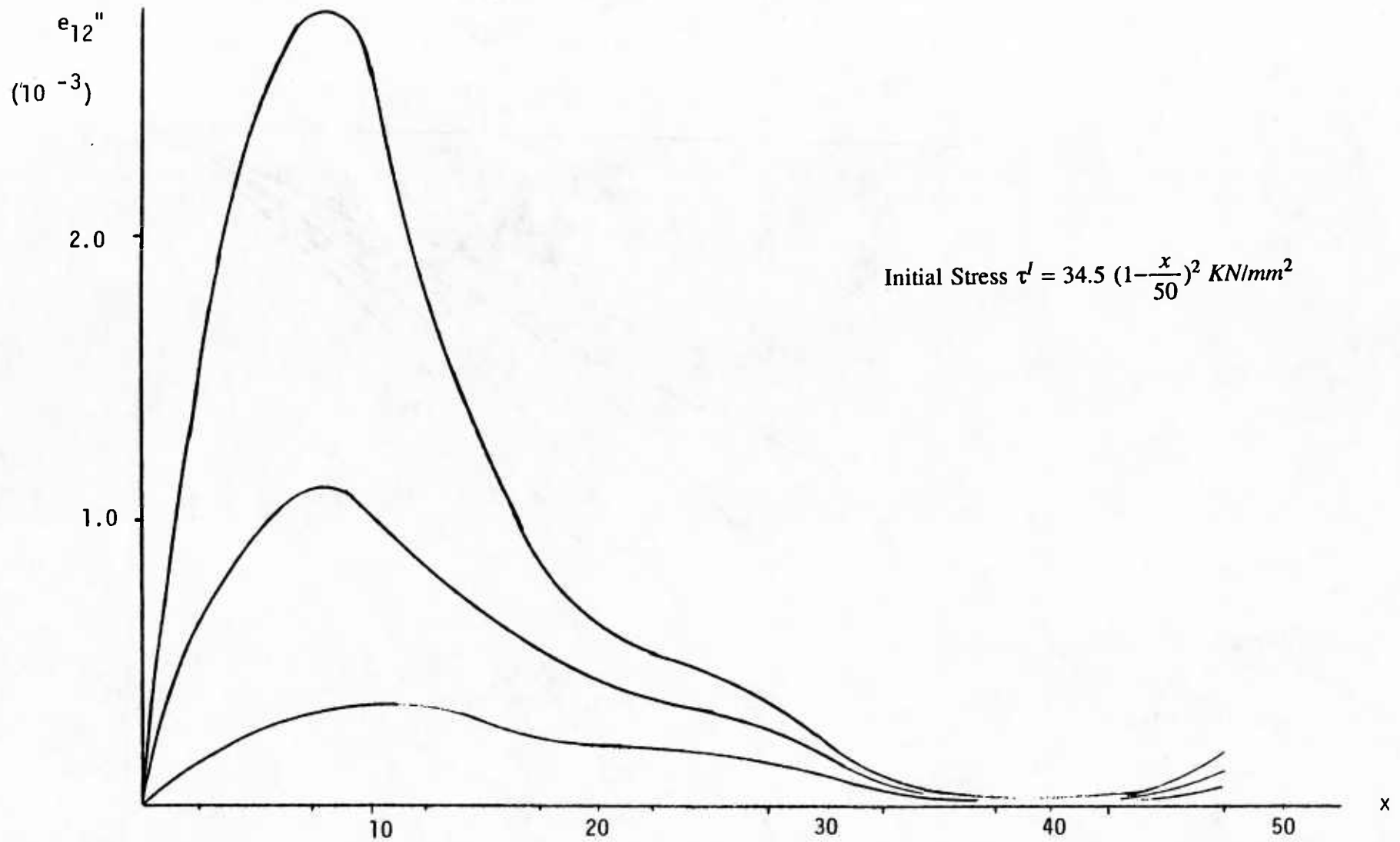


Fig. 7. Plastic Strain Distribution e''_{12} in R



Distance from free surface in microns

Fig. 8 - Plastic Distribution e''_{12} in R.



21

Distance from free surface in microns

Fig. 9 - Plastic Strain Distribution $e''_{\alpha\beta}$ in P,Q.

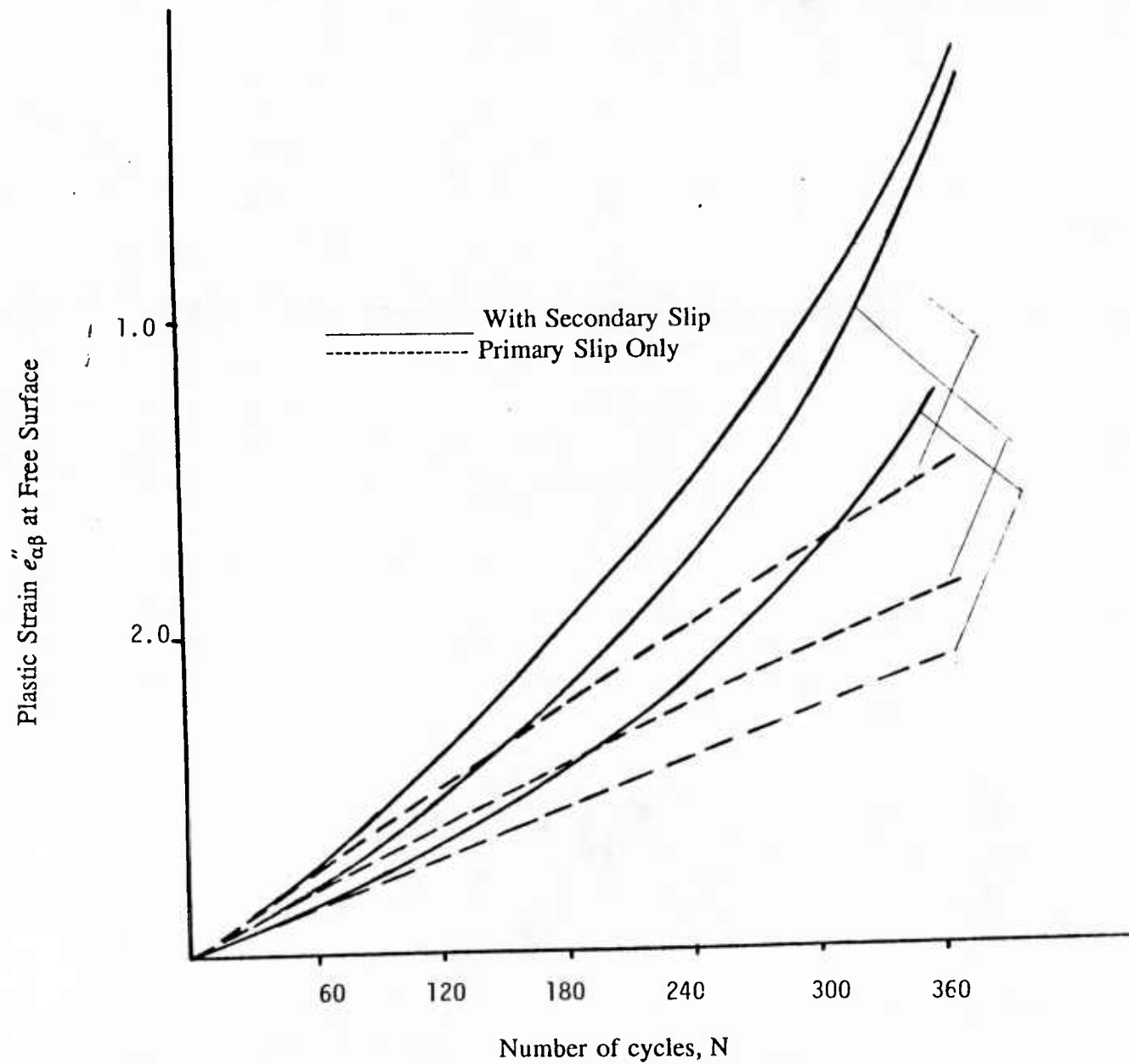


Fig. 10 - Growth of Plastic Strain at Free Surface
With and Without Secondary Slip

$$\tau^I = 3.45 \left(1 - \frac{3x}{250}\right) \text{ KN/m}^2$$

$$\tau^I = 3.45 \left(1 - \frac{x}{50}\right) \text{ KN/m}^2$$

$$\tau^I = 3.45 \left(1 - \frac{x}{50}\right)^2 \text{ KN/m}^2$$

equations in the form (17) equals the number of unknowns of $(\delta e'')$'s in Q and R. These $\delta e''$'s were thus determined. The number of cycles, n, for each extrapolation was 10 cycles. The results for the first extrapolation were compared with those calculated cycle by cycle and the agreement was found to be good.

Some Related Metallurgical Observations

A number of metallurgical observations supporting the micromechanic theory of fatigue crack initiation have been shown by Lin (1977, 1981, 1984). Some metallurgical observations by Mughrabi (1983), related to the present study, are given as follows:

1. The persistent slip bands PSB in pure f.c.c. metals consist of more or less equally spaced dislocation walls, which are densely packed with edge dislocation dipoles and which are separated by so called channels of low dislocation density. These dislocation dipoles can cause different initial shear stresses of opposite signs in P,Q. Three sets of initial stresses are here shown.
2. Single copper crystal fatigue tests show that the extrusion height has exceeded the static extrusion by a large amount. As indicated by Mughrabi these observations do not support the simple theory of the termination of extrusion growth after extrusion height reaches the static extrusion. The rate of growth does not depend markedly on temperature, and the absence of this dependence suggests that some micromechanics process, as proposed here, seems to be the cause of extrusion growth beyond the static extrusion.
3. TEM (Transmission Electron Microscope) observations show that late in the fatigue test, increasing secondary slip activity in the PSB's gradually transforms the primary edge dislocation PSB walls into a cell structure. This shows that secondary slip occurs.

4. The extrusion height in a copper polycrystal of a grain size of $25\ \mu$ was estimated to reach 0.1μ to 0.2μ , indicated by Mughrabi (1983). For a 0.035μ thickness of slices P,Q, used in the present calculation, a $e''_{\alpha\beta}$ of about 2.8 will yield an extrusion of height of 0.1μ . The calculated $e''_{\alpha\beta}$ at the free surface about 1.5. It is expected that increase of loading cycles can yield a $e''_{\alpha\beta}$ of 2.8.

Conclusions

Three thin adjacent slices P,R,Q, in a crystal at the free surface with initial resolved shear stress of opposite signs in P,Q were assumed in a polycrystal. This polycrystal was subjected to cyclic tension and compression loading. Primary slip in P,Q induces a tensile stress and a resolves shear stress in a secondary slip system in R. When the shear stress reaches critical, this secondary slip system slides and gives plastic shear strain e''_{12} which has a strain component $e''_{\alpha\alpha}$. The $e''_{\alpha\alpha}$ has the same effect in causing the initial stress of opposite signs in P,Q as the initial inelastic tensile strain $e'_{\alpha\alpha}$ which may be caused by interstitial dislocation dipoles, shown by Lin Ito [22] and Lin and Lin [18]. Hence, the secondary slip causes the primary slip to proceed further. $e''_{\alpha\alpha}$ contributes to the extrusion growth beyond the initial static extrusion. The same reasoning can be applied to intrusion growth by an array of vacancy dipoles instead of the interstitial ones. After the intrusion is developed to a certain size, the stress concentration will contribute to the crack initiation.

Acknowledgement

This research was supported by the Office of the Naval Research through contract N00014-86-K0153. This support and the interest of the Scientific Officer Dr. Y. Rajapakse are gratefully appreciated.

References

1. McCommon, R.D., and Rosenberg, H.M., "The Fatigue and Ultimate Tensile Strengths of Metals" between 4.2°K and 293°K, *Proc. Roy. Soc. (London)*, Vol. 242A, p. 203, 1957.
2. MacCone, R.K., R.D. MaCommon, and Rosenberg, H.M., "The Fatigue of Metals" at 1.7°K, *Phil. Mag.*, Vol. 4, p. 267, 1959.
3. Forsyth, P.J.E., and Stubbington, C.A., "The Slip Band Extrusion Effect Observed in Some Aluminum Alloys Subjected to Cyclic Stresses," *J. Inst. Metals*, Vol. 83, p. 395, 1955.
4. Thompson, N., N.J. Wadsworth and N. Louat, "The Origin of Fatigue Fracture in Copper," *Phil. Mag.*, Vol. 1, p. 113, 1955.
5. Hull, D., "Surface Structure of Slip Bands on Copper Fatigued" at 293°, 90°, 20° and 4.2°K, *J. Inst of Metals*, Vol. 1, p. 113, 1955.
6. Meke, K. and C. Blochwitz, "Internal Displacement of Persistent Slip Bands in Cyclically Deformed Nickel Single Crystals," *Phys. Stat. Sol. (a)* 61 p. 5, 1980.
7. Maghrabi, H., "Microscopic Mechanisms of *Metals Fatigue Strength of Metals and Alloys*, Vol. 3, Pergamon Press. Oxford and New York, 1980.
8. Mott, N.F., "Origin of Fatigue Cracks," *ACTA Metallurgica*, Vol. 6, p. 195, 1958.
9. Cotterell, A.H. and Hull. D., "Extrusions and Intrusions by Cyclic Slip in Copper," *Proc. Roy. Soc. (London)*, Vol. 242A, p. 211, 1957.
10. Thompson, N., *Proc. Int. Conf. on the Atomic Mechanisms of Fracture*, Technology Press MIT and John Wiley & Sons, 1959.
11. Kennedy, A.J., "*Processes of Creep and Fatigue in Metals*, John Wiley & Sons, Inc., 1963.
12. McEvily, J., Jr. and Machlin, E.S., "Critical Experiments on the Nature of Fatigue in Crystalline Materials," *Proc. Int. Conf. on the Atomic Mechanism of Fracture*, Technology Press, MIT and John Wiley & Sons, 1959.
13. Wood, W.A., "*Mechanism of Fatigue*," *Fatigue in Aircraft Structures* (Edited by A.M. Freudental), Academic Press, New York, 1956, pp. 1-19.
14. Lin, T.H., and M. Ito, "Mechanism of a Fatigue Crack Nucleation Mechanism," *J. Mech. Phys. Solids*, Vol. 17, pp. 511-523, 1969.
15. Lin. T.H., "Micromechanic of Fatigue Crack Initiation: Theory and Experimental Observations," *Mechanics of Fatigue - AMD*, Vol. 47, ASME, Edited by T. Mura, pp. 41-109, 1981.
16. Lin. S.R., and T.H. Lin, "Initial Strain Field and Fatigue Crack Initiation Mechanics," published in *J. Appl. Mech.*, Vol. 50, pp. 367-372, 1987.

17. Taylor, G.I., "Plastic Deformation of Metals," *J. Inst. Metals*, Vol. 62, p. 307, 1938.
18. Parker, E.R., *Mechanical Behavior of Materials in Elevated Temperatures*, Dorn, J.E. ed., McGraw-Hill, New York, pp. 129-148.
19. Lin, T.H. *Theory of Inelastic Structures*, pp. 43-55, John Wiley & Sons, 1968.
20. Lin, T.H. and M. Ito, "Theoretical Plastic Stress-Strain Relationship of a Polycrystal and Comparisons with Von Mises and Tresca's Plasticity Theories," *J. Engineering Science*, Vol. 4, p. 543-561, 1966.
21. Eshelby, J.D., "The Determination of the Elastic Field of an Ellipsoidal Inclusion and Related Problems," *Proc. Roy. Soc., A* Vol. 241, p. 396.
22. Lin, T.H. and Y.M. Ito, 1969, "Fatigue Crack Initiation in Metals." *Proc. U.S. Nat. Acad. Sc.*, Vol. 62, No. 3, pp. 631-635.
23. Essmann, V., V. Gosele and H. Mughrabi, 1981, "A Model of Extrusions and Intrusions in Fatigue Metals," *Phil. Mag.* Vol. 44, No. 2, pp. 405-420.
24. Mughrabi, H., 1980, "Microscopic Mechanisms of Metal Fatigue," *Strength of Metals and Alloys*, Vol. 3, Pergamon Press, Oxford and New York, pp. 1615-1638.
25. Mughrabi, H., R. Wang, K. Differt and V. Essmann, " 1983, "Fatigue Crack Initiation by Cyclic Slip Irreversibilities in High Cycle Fatigue," ASTM STP 811, Fatigue Mechanisms.
26. Lin, S.R. and T.H. Lin, 1974, "Effect of Secondary Slip Systems on Early Fatigue Damage," *J. Mech. Phys. Solids*, Vol. 22, pp. 171-191.
27. Lin, S.R., 1971, "Effect of Secondary Slip on Early Fatigue Damage," Ph.D. Dissertation, UCLA.
28. Lin, S.R. and T.H. Lin, 1984, "Initial Strain Field and Fatigue Crack Initiation Mechanics." *J. Appl. Mech.*, Vol. 50, pp. 367-372.

U232686